Annals of Diagnostic Pathology 38 (2019) 80–86

Contents lists available at ScienceDirect

Annals of Diagnostic Pathology

journal homepage: www.elsevier.com/locate/anndiagpath

Papillary pattern in clear cell renal cell carcinoma: Clinicopathologic, morphologic, immunohistochemical and molecular genetic analysis of 23 cases

Reza Alaghehbandan[a], Monika Ulamec[b], Petr Martinek[c], Kristyna Pivovarcikova[c], Kvetoslava Michalova[c], Faruk Skenderi[d], Milan Hora[e], Michal Michal[c], Ondrej Hes[c,*]

[a] Department of Pathology, Faculty of Medicine, University of British Columbia, Royal Columbian Hospital, Vancouver, BC, Canada
[b] "Ljudevit Jurak" Pathology Department, Clinical Hospital Center "Sestre milosrdnice", Pathology Department, Medical University, Medical Faculty, Zagreb, Croatia
[c] Department of Pathology, Charles University, Faculty of Medicine in Plzeň, Pilsen, Czech Republic
[d] Department of Pathology, University of Sarajevo Clinical Center, Sarajevo, Bosnia and Herzegovina
[e] Department of Urology, Charles University, Faculty of Medicine in Plzeň, Pilsen, Czech Republic

ARTICLE INFO

Keywords:
Clear cell renal cell carcinoma
Papillary pattern
NGS

ABSTRACT

Clear cell renal cell carcinoma (ccRCC), the most common histologic subtype of RCCs, demonstrates a wide spectrum of morphologic features (i.e., low-grade spindle cell, syncytial giant cells, and mucin-producing cells). However, papillary growth pattern in ccRCCs is rather a rare finding, which can present challenges in differential diagnostic work up. The aim of this study was to investigate ccRCCs with predominant papillary features from morphologic, immunohistochemical and molecular genetic perspectives.

23 clear cell renal cell carcinomas with papillary architecture were selected. Tumors were evaluated morphologically, immunohistochemically, and molecularly by next-generation sequencing (NGS). The diagnosis of MiT family translocation RCC was excluded by TFE3 immunohistochemistry.

Mean age of patients was 65.2 years (range 42–81 years), and 19/23 were male. Tumor size ranged from 1.6 to 12.8 cm (median 6.5 cm). At a median follow-up of 2.5 years (range 1.5–9 years), 2 patients (8.7%) died of disease, 2 developed metastasis. Areas of papillary pattern accounted for approximately 40–100% of the tumor. CK7 was negative in non-papillary areas in majority of cases (20/23, 87%), and was only focally positive in 3/23 cases (13%). In papillary areas, AMACR was positive/focally positive in 17/23 (73.9%) cases and in the non-papillary areas it was positive/focally positive in 22/23 (95.6%) cases. CAIX was mainly negative in both non-papillary and papillary areas (15/23 [65%] and 16/23 [69.5%], respectively). Molecular analysis of 15 analyzable cases revealed the most frequently mutated gene to be *VHL* (in 9 cases), followed by *PRBM1* (in 2 cases) and 29 other different mutations in various genes.

Papillary growth pattern in ccRCC is not an uncommon situation. Papillary RCC with clear cells and MiT family (TFE3) translocation RCCs are the major differential diagnostic considerations in such scenarios. Our NGS molecular analysis supported classifying such tumors as a morphologic variant of ccRCC.

1. Introduction

Clear cell renal cell carcinoma (ccRCC) is the most common subtype of RCCs, representing approximately 65–70% of all adult renal carcinomas [1]. ccRCCs are architecturally and cytologically diverse including solid, alveolar, acinar, cystic growth patterns of neoplastic cells with clear and/or eosinophilic cytoplasm. High-grade ccRCCs usually composed of mixed neoplastic cells with clear and eosinophilic cytoplasm. In fact, tumor heterogeneity is a well-documented and known phenomenon in ccRCCs with various morphologic features such as low-grade spindle cell, syncytial giant cells, and mucin-producing cells [2-5]. The presence of mixed morphologic components in renal neoplasms in general and in ccRCCs in particular can be puzzling in routine practice, which can potentially lead to misdiagnosis [6].

It is well-known that ccRCCs can present with papillary architectural growth pattern although rarely. A number of studies since early 1990s studied and reported RCCs with clear cells and papillary features [7-10]. This finding is not rare and certainly can pose diagnostic

* Corresponding author at: Department of Pathology, Medical Faculty, Charles University Hospital Plzen, Alej Svobody 80, 304 60 Pilsen, Czech Republic.
E-mail address: hes@medima.cz (O. Hes).

https://doi.org/10.1016/j.anndiagpath.2018.11.004

Table 1
Clinicopathologic data on patients with clear cell renal cell carcinoma with papillary architecture.

Case	Papillary (%)	Classic clear cell (%)	Necrosis (%)	No. block	Gender	Age	Size (cm) +	pTNM	Grade	Follow up (mon)
1	100	0	0	2	F	57	6	T3aNxMx	3	2 yrs AW, then LF
2	80	15	5	2	M	77	5.2	T1b	3	LF
3	60	40	0	3	M	62	8	T3a	3	3 yrs WA
4	70	30	0	2	M	74	7.5	T2NxM1[a]	3	1.5 yrs DOD
5	85	0	40	2	M	54	6.5	T1bNxMx	4	2.3 yrs DOD[b]
6	75	25	0	2	M	76	3.3	T1a	3	5 yrs AW
7	60	40	5	10	M	42	7.5	T3aNx	4	1.5 yrs AW
8	70	20	10	6	F	81	4.5	T3aN0Mx	3	AW 2 years
9	85	10	15	2	M	81.	7	T3b	3	LF
10	90	5	5	5	M	76	5,5	pT1b	2	LF
11	60	40	0	2	M	54	3	T1a	3	LF
12	60	20	20	6	M	64	8	T3bN0Mx	4	6 yrs AW, then LF
13	40	60	0	4	M	61	3.5	T1a	2	9 yrs AW
14	80	10	10	4	M	68	4	T1b	3	LF
15	95	5	0	4	F	58	4	pT1b	1	9 yrs AW[c]
16	70	25	5	3	M	48	9	pT3b	3	LF
17	70	30	3	1	M	69	3	pT1a	3	LF
18	80	20	0	1	M	56	1.6	pT1a	2	5 yrs AW[e]
19	100	0	0	1	M	67	8	pT2a	2	2 years AW[f]
20	75	5	50	2	M	67	12.5	pT3	2	2.5 yrs AW, then DotD[d]
21	70	30	0	1	F	65	4.5	pT1b	3	LF
22	50	50	10	11	M	74	8	pT3a	3	LF
23	60	20	20	5	M	63	12.8	pT3a	3	LF

DotD = dead of other disease, DOD = dead of disease, AW = alive and well, LF = lost to follow up, M = male, F = female, + = largest diameter, yr = year, yrs = years.

[a] Meta to lung, vertebra.
[b] Meta to brain, lung, lymph nodes, liver.
[c] Treated for breast carcinoma.
[d] Myocardial infarct.
[e] Followed for cataract.
[f] Surgery for cataract.

challenge in limited samples (i.e., renal core biopsies). The differential diagnosis would include two main RCC subtypes, namely papillary RCC and ccRCC with papillary features. The recent 2016 WHO (World Health Organization) classification included RCCs with clear cell features such as clear cell papillary RCC and MiT family translocation carcinomas (namely Xp11.2) [1]. This differential diagnosis can have potential therapeutic implications and as such it would be crucial to arrive in accurate diagnosis.

The purpose of this study was to investigate ccRCCs with predominant papillary features from morphologic, immunohistochemical and molecular genetic perspectives. It is our hope that findings of this study will shed light on better understanding of such neoplasms.

2. Materials and methods

An institutional Ethics Review was obtained for the study. Cases were selected and retrieved by searching both in-house and consultation files of Charles University Hospital, Plzen, Czech Republic, and the Royal Columbian Hospital, University of British Columbia, Canada.

Of 543 ccRCCs searched, 23 were selected which included ccRCCs with prominent papillary architecture (more than 40%). All cases were reviewed by two urologic pathologists (R.A. and O.H.). One or multiple blocks/slides were available for review in all cases (ranging from 1 to 11). Clinicopathologic and follow-up data were collected using medical chat review and contacting primary consulting pathologists in all cases. The diagnosis of MiT family translocation RCC was excluded by TFE3 immunohistochemistry.

Tissues for light microscopy were fixed in 4% formaldehyde and embedded in paraffin using a routine procedure. 5 μm thick sections were cut from the tissue blocks and were stained with hematoxylin and eosin.

2.1. Immunohistochemical studies

The immunohistochemical study was performed using a Ventana Benchmark XT automated stainer (Ventana Medical System, Inc., Tucson, AZ, USA). Immunochemical studies were carried out using a panel of antibodies including CK7 (OV-TL12/30, monoclonal, DakoCytomation, Carpinteria, CA, 1:200), racemase/AMACR (P504S, monoclonal, Zeta, Sierra Madre, CA, 1:50), vimentin (D9, monoclonal, NeoMarkers, Westinghouse, CA, 1:1000), carbonic anhydrase IX (rhCA9, monoclonal, RD systems, Abingdon, GB, 1:100), TFE3 (polyclonal, Abcam, Cambridge, UK, 1:100), and CD10 (monoclonal 56C6, Leica, Newcastle, UK, 1:20). Appropriate positive and negative controls were used.

2.2. NGS mutation analysis

A panel of 271 cancer related genes (Comprehensive Cancer Panel, Qiagen, Hilden, Germany) was used to analyze tumor tissue samples. The samples were isolated using macro dissection from FFPE blocks. DNA was isolated using Qiagen DNA mini kit, and 250 ng of DNA was used to construct the library. The QIAseq technology applies unique Molecular Identifiers (UMI) for more specific allele frequency determination as well as PCR error reduction. Technical duplicates and positive controls were used to establish quality control of the analysis parameters. Library was sequenced on Illumina's Nextseq 500, aiming at average coverage 350× after deduplication of molecular identifiers to detect 10% allele frequency with 95% sensitivity. Variants were called using Qiagen's proprietary pipeline. Subsequently the variants were filtered using the calculated limit of detection for each sample. Furthermore the variants were annotated using The Genome Aggregation Database (GnomAD) [11] for population statistics and ClinVar database [12] for the relationships among variations and phenotypes. Variants more frequent than 0.001% in the GnomAD database were excluded as well as known benign variants according to the

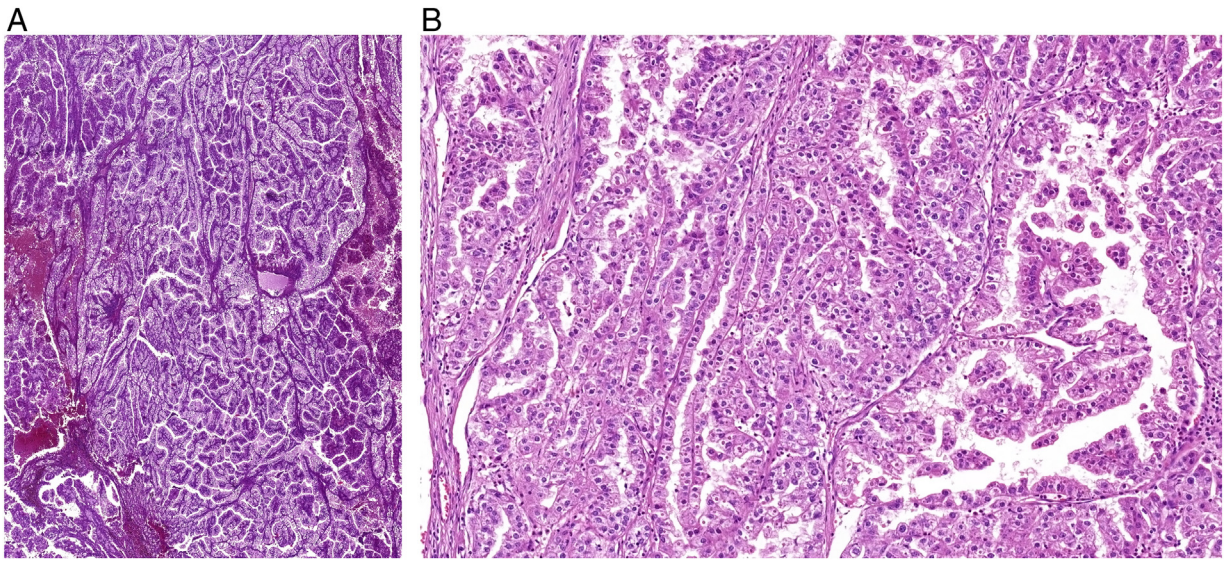

Fig. 1. a. Clear cell renal cell carcinoma with prominent papillary pattern.
b. Clear cell renal cell carcinoma with areas of compressed papillary structures.

ClinVar database. The remaining subset was checked visually, and suspected artefactual variants were excluded.

3. Results

Table 1 presents clinical and demographic information on 23 patients including 19 males and 4 females. Patient's age ranged from 42 to 81 years (mean 65.2, median 65 years). Tumor size varied from 1.6 to 12.8 cm (mean 6.3, median 6.5 cm). Follow up data (1.5–9 years, mean 3.9, median 2.5 years) were available in 13 of 23 patients. Eleven patients were staged as pT1, 2 patients pT2, and 10 patients pT3. Metastases were documented in 2 cases. Two patients died of disease (1.5 and 2.3 years after diagnosis).

Gross description was available in 13 cases, showing yellow golden masses with regressive changes, hemorrhages and foci of firm gray tissue on cut surface. Necrotic areas were present in 12 cases, ranging from 5 to 50% of the total tumor volume.

Microscopically, all tumors showed majority of neoplastic cells with predominantly clear cytoplasm, arranged mainly in alveolar, nested, and trabecular patterns, separated by fibrovascular septae. Areas of papillary pattern accounted for approximately 40–100% of the tumor (Fig. 1a–b). Papillae were lined by clear and/or eosinophilic neoplastic cells (Fig. 2a–b). Foamy macrophages were not observed. The ISUP/WHO histologic grade ranged 1–4 (Fig. 3a–c).

Results of immunohistochemical examination are summarized in Table 2. CK7 was negative in non-papillary areas in majority of cases (20/23, 87%), and was only focally positive in 3/23 cases (13%). In papillary areas, AMACR was positive/focally positive in 17/23 (73.9%) cases and in the non-papillary areas it was positive/focally positive in 22/23 (95.6%) cases. CAIX immunohistochemical stain was mainly negative in both non-papillary and papillary areas (15/23 [65%] and 16/23 [69.5%], respectively). On the other hand, vimentin was positive/focally positive in most cases in both non-papillary and papillary areas (20/23 [87%] and 18/23 [78.3%], respectively). CD10 immunohistochemical stain was consistently positive (either focal or diffuse) in non-papillary area (23/23, 100%), and similarly it was positive in 22/23 (95.6%) cases in the papillary area. TFE3 was negative in all 23 cases.

Fifteen of 23 samples were successfully sequenced (met the quality control standards) and as a result, a total of forty mutations were filtered (Table 3). Most frequently mutated gene was *VHL* (in 9 cases) followed by *PRBM1* (in 2 cases) and 29 other different mutations in various genes. Some samples with low DNA quality had unfavourable ratio of sequenced reads to UMI's and as such the limit of detection was increased. The details are listed in Table 4.

4. Discussion

ccRCC usually shows a solid, alveolar or acinar growth pattern, composed of clear or eosinophilic neoplastic cells. Tumor heterogeneity in renal neoplasms is a well-documented fact [6,13]. ccRCC, the most common subtype of RCCs, are no exception and can exhibit great variability in both architectural growth patterns and morphologic features. The morphologic features of ccRCCs can also be dependent on the tumor grade, with higher tumor grades demonstrating a mixture of clear cells and neoplastic cells with eosinophilic granular cytoplasm. In fact, our group recently described a rare subset of high grade ccRCCs with prominent emperipolesis [14]. These tumors showed focal pseudopapillary features with large cells with bizarre nuclei and eosinophilic rhabdoid-like cytoplasm [14]. In recent years, a number of rare morphologic variants of ccRCCs have been described, including mucin-secreting ccRCC, ccRCC with low-grade spindle cell proliferation, ccRCC with syncytial giant cell component, and ccRCCs with prominent emperipolesis [2,4,5,14,15].

From architectural point of view, although ccRCCs usually present in a solid growth pattern, cystic changes can frequently be seen. ccRCC with true papillary architecture is a rather rare variant but has previously been described [7-10,16]. According to the most recent World Health Organization (WHO) Classification of Genitourinary tumors, “focal” papillary areas can be seen in ccRCCs [17]. In reality, we and others have noticed that ccRCCs can have rather large papillary areas with well-formed true papillae [7-10,16]. In fact, the papillary area could constitute a substantial portion of the tumor as it is the case in our study with ccRCCs demonstrating between 40 and 100% papillary areas. This can simply present a diagnostic challenge in routine practice, particularly in limited samples, with the current understating that ccRCCs can have “focal” papillary areas [17]. The two most common differential diagnoses of RCCs with papillary architecture and clear cell morphology would include MiT family (TFE3) translocation RCC, and clear cell papillary RCC. Other rather less frequent differential diagnoses would include collision tumors, *fumarate hydratase*-deficient RCCs, and RCCs with leiomyomatous stroma [18]. It would be expected that such tumors might have been classified as PRCC, collision tumors, or even unclassified in the past [9,10]. However, with the current

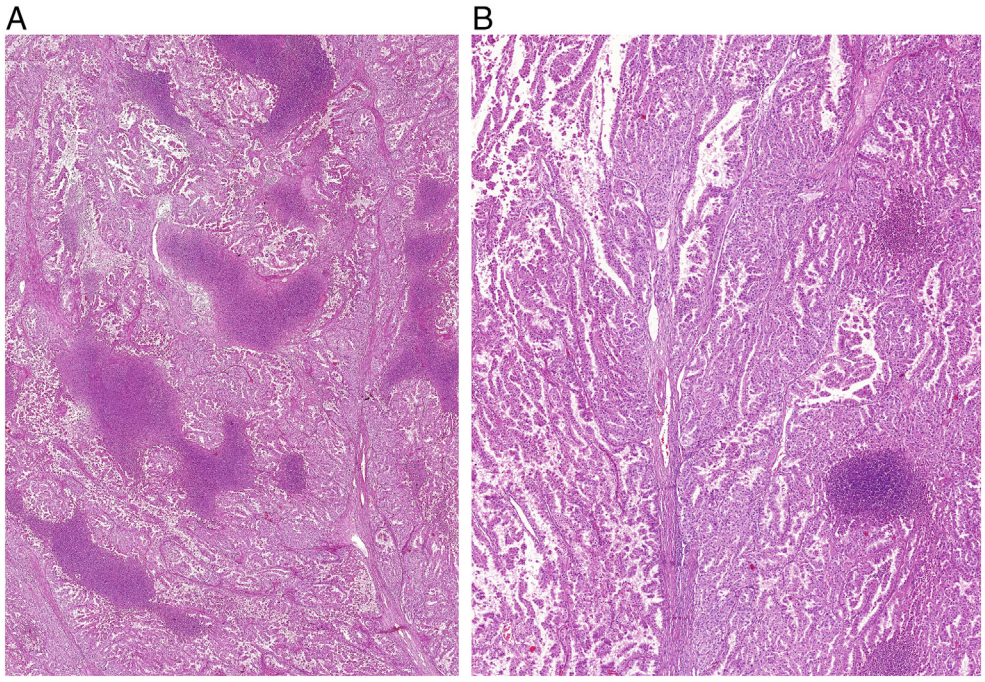

Fig. 2. a. Clear cell renal cell carcinoma with papillary pattern and extensive foci of necrosis.
b. Clear cell renal cell carcinoma with papillary architecture and small foci of necrosis.

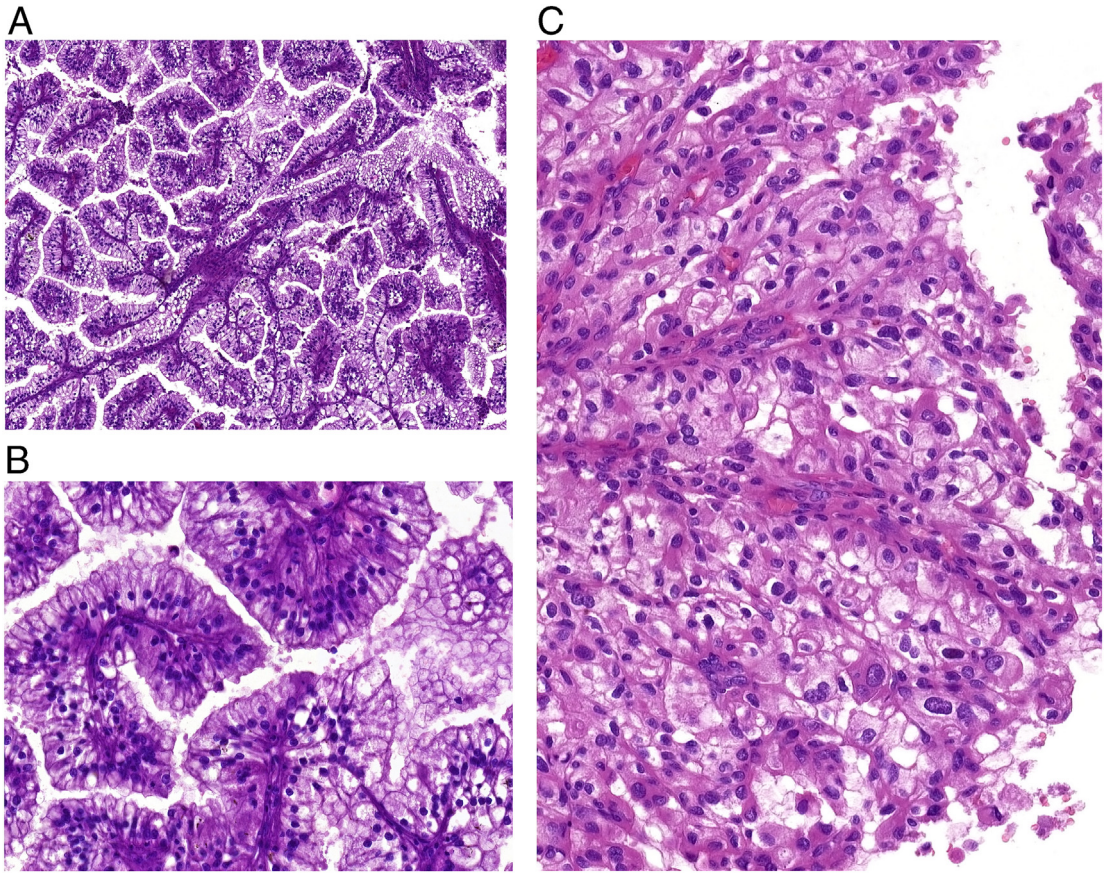

Fig. 3. a. Cytological features are identical to clear cell renal cell carcinoma, however demonstrating papillary architecture.
b. Clear cell renal cell carcinoma with papillary features showing grade 1 nuclear grade.
c. Clear cell renal cell carcinoma with papillary features showing grade 3 nuclear morphology.

Table 2
Results of immunohistochemistry on clear cell renal cell carcinoma with papillary architecture.

Case	CK7-cc	CK7-Pap	AMACR-cc	AMACR-Pap	CAIX-cc	CAIX-Pap	Vim-cc	Vim-Pap	CD10-cc	CD10-Pap	TFE3 cc/Pap
1	Neg.	Neg.	Neg.	Focal pos.	Neg.	Neg.	Focal pos.	Focal pos.	Pos.	Pos.	Neg.
2	Neg.	Neg.	Neg.	Focal pos.	Neg.	Neg.	Focal pos.	Focal pos.	Pos.	Pos.	Neg.
3	Neg.	Neg.	Focal pos.	Pos.	Pos.	Pos.	Pos.	Focal pos.	Pos.	Pos.	Neg.
4	Neg.	Focal pos.	Neg.	Focal pos.	Neg.	Neg.	Focal pos.	Focal pos.	Pos.	Pos.	Neg.
5	Neg.	Neg.	Focal pos.	Pos.	Neg.	Neg.	Focal pos.	Focal pos.	Focal pos.	Focal pos.	Neg.
6	Neg.	Neg.	Focal pos.	Focal pos.	Neg.	Neg.	Focal pos.	Focal pos.	Pos.	Pos.	Neg.
7	Neg.	Neg.	Focal pos.	Focal pos.	Focal pos.	Focal pos.	pos.	Pos.	Pos.	Pos.	Neg.
8	Focal pos.	Neg.	Pos.	Pos.	Neg.	Neg.	Focal pos.	Focal pos.	Pos.	Pos.	Neg.
9	Neg.	Neg.	Pos.	Pos.	Focal pos.	Neg.	Focal pos.	Neg.	Pos.	Pos.	Neg.
10	Neg.	Neg.	Focal pos.	Focal pos.	Neg.	Neg.	Focal pos.	Focal pos.	Pos.	Pos.	Neg.
11	Focal pos.	Neg.	Pos.	Focal pos.	Neg.	Neg.	pos.	Focal pos.	Pos.	Focal pos.	Neg.
12	Focal pos.	Pos.	Focal pos.	Focal pos.	Neg.	Neg.	Neg.	Neg.	Focal pos.	Pos.	Neg.
13	Neg.	Neg.	Focal pos.	Focal pos.	Pos.	Pos.	Pos.	Pos.	Pos.	Pos.	Neg.
14	Neg.	Neg.	Pos.	Pos.	Neg.	Neg.	pos.	Neg.	Pos.	Pos.	Neg.
15	Neg.	Neg.	Focal pos.	Focal pos.	Neg.	Neg.	Focal pos.	Focal pos.	Pos.	Neg.	Neg.
16	Neg.	Neg.	Focal pos.	Focal pos.	Neg.	Neg.	Neg.	Neg.	Pos.	Pos.	Neg.
17	Neg.	Neg.	Focal pos.	Focal pos.	Pos.	Pos.	Focal pos.	Focal pos.	Pos.	Focal pos.	Neg.
18	Neg.	Neg.	Neg.	Focal pos.	Neg.	Neg.	Pos.	Pos.	Pos.	Pos.	Neg.
19	Neg.	Neg.	Focal pos.	Pos.	Neg.	Neg.	Neg.	Neg.	Pos.	Pos.	Neg.
20	Neg.	Neg.	Pos.	Pos.	Neg.	Neg.	Focal pos.	Focal pos.	Pos.	Focal pos.	Neg.
21	Neg.	Focal pos.	Focal pos.	Focal pos.	Focal pos.[a]	Focal pos.[a]	Pos.	Pos.	Pos.	Pos.	Neg.
22	Neg.	Neg.	Neg.	Neg.	Pos.	Pos.	Pos.	Pos.	Pos.	Pos.	Neg.
23	Neg.	Neg.	Neg.	Focal pos.	Pos.	Pos.	Pos.	Pos.	Pos.	Focal pos.	Neg.

cc = classic clear cell area, Pap = papillary area, Neg. = negative, Pos. = positive, CAIX = carbonic anhydrase 9, vim = vimentin.
[a] Artefact/fixation.

Table 3
Summary of molecular genetic findings on analyzable clear cell renal cell carcinoma with papillary architecture.

Case	HCCP # mutations	LOD 95
1	NA	NA
2	7	0.1301
3	5	0.0949
4	5	0.1881
5	4	0.2144
6	1	0.3418
7	NA	NA
8	0	0.1961
9	1	0.4606
10	NA	NA
11	0	0.5108
12	NA	NA
13	3	0.1197
14	1	0.4389
15	NA	NA
16	2	0.192
17	3	0.192
18	2	0.1675
19	5	0.0575
20	1	0.1843

HCCP # mutations – human comprehensive cancer panel result with number of detected variants, LOD 95 – average 95th percentile estimated minimum detectible allele fraction, NA not analyzable.

knowledge and available ancillary testing such tumors can hopefully be correctly diagnosed.

MiT family (TFE3) translocation RCCs, mostly tumors associated with Xp11.2 translocation, demonstrate variable morphological features. These tumors are mostly arranged in papillary architecture with large, weakly eosinophilic or clear neoplastic cells with occasional psammoma bodies and eosinophilic hyaline nodules. Immunohistochemically, these tumors express TFE3 protein, albeit TFE3 break-apart fluorescence in situ hybridization assay is the most reliable method of detection [18]. Clear cell papillary RCC, the other main differential diagnosis, is easily recognizable morphologically, including tubopapillary architecture, variable presence of leiomyomatous stroma, “shark smiles,” and apical “blister” feature and low-grade basally located nuclei. Unlike ccRCCs which are mostly CK7 negative/focally positive, these tumors are strongly and diffusely positive for CK7 [18].

Earlier studies including Fuzesi et al. [16] analyzed 3 cases of PRCC with clear cell morphology, using classic cytogenetics (standard G-banding techniques), which demonstrated loss of terminal 3p chromosomal segments with no trisomy 17 observed. Subsequently, Salama et al. [7] used fluorescence in situ hybridization (FISH) and microsatellite analysis to determine the genetic alterations in 7 malignant renal tumors with papillary architecture and extensive clear cell change. The authors concluded that because such tumors showed molecular changes identical to ccRCCs, such neoplasms should be classified as ccRCC [7]. Most recently, Jia et al. [19] examined 13 cases of RCCs with clear cytoplasm, high-grade nuclear features, and prominent papillary architecture from Memorial Sloan Kettering Cancer Center and TCGA papillary RCC public databases. The authors reported that molecular analysis of 8 cases revealed a *VHL* mutation and concurrent 3p loss in 7 of 8 cases, while no trisomy 7/17 or MET mutations were found. They concluded that molecular analysis of such neoplasms with clear cytoplasm and prominent papillary architecture showed characteristic molecular features of ccRCC and supports their classification as a rare morphologic variant of ccRCC.

In our study, the samples analyzed by NGS Comprehensive cancer panel showed large variety of variants with mostly unknown pathogenicity (Table 4). Most frequently mutated gene was *VHL* (in 9 cases) followed by *PRBM1* (in two cases) and 29 other different mutations in various genes. Five of the most commonly mutated genes in ccRCCs including *VHL*, *PRBM1*, *PTEN*, *PIK3CA*, and *KDM5C*, were mutated in our study group [20]. It should be noted that most of the low frequency samples were filtered out due to the insufficient limit of detection, which was caused by low quality of source DNA of many samples. The somatic status of the variants was confirmed by comparing tumor to normal tissue pairs. Of note, some variants had no known clinical implication/interpretation. Our molecular genetic findings are compatible with prior studies, particularly with Jia et al. [19], in which such tumors share characteristic molecular features of ccRCC and that they are best classified as a rare morphologic variant of ccRCC.

Table 4
Details of detected mutations on analyzable clear cell renal cell carcinoma with papillary architecture.

Case	pos	Variant frequency	Symbol	HGVSc	HGVSp	VEP dbSNP ID	Clinical significance
2	chr3:10188316	0.2197	*VHL*	NM_000551.3:c.461del	NP_000542.1:p.Pro154GlnfsTer5	CM065515	Pathogenic
	chr3:52643374	0.2206	*PBRM1*	NM_181042.4:c.2522A > C	NP_851385.1:p.Gln841Pro	–	–
	chr4:66270158	0.1839	*EPHA5*	NM_001281765.2:c.1727T > A	NP_001268694.1:p.Ile576Asn	–	–
	chr9:139405209	0.4185	*NOTCH1*	NM_017617.3:c.2636G > A	NP_060087.3:p.Arg879Gln	rs368011392	Uncertain significance
	chr17:8109861	0.5329	*AURKB*	NM_001284526.1:c.637G > C	NP_001271455.1:p.Gly213Arg	rs149651741	–
	chr22:23655142	0.2306	*BCR*	NM_004327.3:c.3391T > C	NP_004318.3:p.Tyr1131His	–	–
	chrX:53245132	0.2439	*KDM5C*	NM_004187.3:c.807del	NP_004178.2:p.Thr270GlnfsTer2	–	Pathogenic
3	chr1:226253407	0.0966	*H3F3A*	NM_002107.4:c.179A > G	NP_002098.1:p.Glu60Gly	–	–
	chr3:10188308	0.2451	*VHL*	NM_000551.3:c.451_452delinsTG	NP_000542.1:p.Ile151Cys	COSM479175	–
	chr3:47098949	0.2118	*SETD2*	NM_014159.6:c.6325C > T	NP_054878.5:p.Arg2109Ter	COSM4970575, COSM4970576	Pathogenic
	chr10:89720679	0.0976	*PTEN*	NM_001304717.2:c.1349C > A	NP_001291646.2:p.Thr450Lys	rs398123329, CM109589, COSM35645, COSM5347081	Uncertain significance
	chr19:52714542	0.2068	*PPP2R1A*	NM_014225.5:c.300G > T	NP_055040.2:p.Glu100Asp	–	–
4	chr3:10183770	0.332	*VHL*	NM_000551.3:c.239G > A	NP_000542.1:p.Ser80Asn	rs5030805, CM961418, CM951273, CD951872, COSM30216, COSM3364919	–
	chr3:52595935	0.2424	*PBRM1*	NM_181042.4:c.4135del	NP_851385.1:p.Arg1379GlyfsTer5	COSM4119134, COSM4119135, COSM4119136	Pathogenic
	chr7:116339762	0.293	*MET*	NM_001127500.2:c.624T > G	NP_001120972.1:p.Asp208Glu	–	–
	chr19:15271577	0.485	*NOTCH3*	NM_000435.2:c.6862C > T	NP_000426.2:p.Pro2288Ser	rs551855907	–
	chrX:123210269	0.6429	*STAG2*	NM_001042749.1:c.2621A > T	NP_001036214.1:p.Tyr874Phe	–	–
5	chr3:10188196	0.2756	*VHL*	NM_000551.3:c.341-2A > T	–	CS071275, COSM14425, COSM17750, COSM30295	Pathogenic
	chr3:178936091	0.2899	*PIK3CA*	NM_006218.2:c.1633G > A	NP_006209.2:p.Glu545Lys	rs104886003, CM126692, COSM125370, COSM27133, COSM295672, COSM763	Pathogenic/likely pathogenic
	chr6:117647551	0.3696	*ROS1*	NM_002944.2:c.5393A > G	NP_002935.2:p.Asn1798Ser	–	–
	chr9:98009767	0.6316	*FANCC*	NM_000136.2:c.197C > T	NP_000127.2:p.Thr66Ile	rs762234072	–
6	chr2:46597010	0.4825	*EPAS1*	NM_001430.4:c.824G > A	NP_001421.2:p.Arg275His	rs759634197, COSM461020	–
9	chr7:6026906	0.5043	*PMS2*	NM_001322014.1:c.1490G > A	NP_001308943.1:p.Gly497Asp	rs199739859, COSM3412219	Conflicting interpretations of pathogenicity
13	chr1:65321324	0.4789	*JAK1*	NM_001321853.1:c.1516C > T	NP_001308782.1:p.Arg506Cys	rs61735631	Not provided
	chr2:178098806	0.15	*NFE2L2*	NM_006164.4:c.239C > G	NP_006155.2:p.Thr80Arg	COSM132857, COSM132861, COSM132964	–
	chr3:10183739	0.4194	*VHL*	NM_000551.3:c.208G > T	NP_000542.1:p.Glu70Ter	rs5030802, CM951268, CM984688, COSM1169478, COSM17711	Pathogenic
14	chr10:8111553	0.4444	*GATA3*	NM_001002295.1:c.1042C > T	NP_001002295.1:p.Leu348Phe	COSM4603687	–
16	chr3:10191508	0.6216	*VHL*	NM_000551.3:c.504_508del	NP_000542.1:p.Leu169GlnfsTer3	–	Pathogenic
	chr14:103363665	0.3125	*TRAF3*	NM_145725.2:c.887G > A	NP_663777.1:p.Cys296Tyr	–	–
17	chr3:10191546	0.2899	*VHL*	NM_000551.3:c.541_550del	NP_000542.1:p.Val181SerfsTer18	–	Pathogenic
	chr15:91346808	0.4231	*BLM*	NM_000057.2:c.3416G > C	NP_000048.1:p.Arg1139Pro	rs771776126, COSM5850071	Uncertain significance
	chr19:42791037	0.2751	*CIC*	NM_001304815.1:c.2909C > T	NP_001291744.1:p.Pro970Leu	–	–
18	chr3:10188252	0.3846	*VHL*	NM_000551.3:c.395A > C	NP_000542.1:p.Gln132Pro	CM994242, COSM17857	–
	chr3:69987012	0.7264	*MITF*	NM_198159.2:c.394C > A	NP_937802.1:p.Gln132Lys	rs201297175	–
19	chr3:10191572	0.2045	*VHL*	NM_000551.3:c.567del	NP_000542.1:p.Asp190ThrfsTer12	–	Pathogenic
	chr5:149433662	0.1211	*CSF1R*	NM_005211.3:c.2889G > C	NP_005202.2:p.Leu963Phe	–	–
	chr9:98222010	0.2051	*PTCH1*	NM_000264.3:c.2759A > C	NP_000255.2:p.Tyr920Ser	–	–
	chr12:46123671	0.1032	*ARID2*	NM_152641.2:c.52G > A	NP_689854.2:p.Ala18Thr	–	–
	chr16:89846345	0.5191	*FANCA*	NM_000135.2:c.1647G > C	NP_000126.2:p.Gln549His	–	–
20	chr16:2110710	0.4205	*TSC2*	NM_000548.4:c.1015G > A	NP_000539.2:p.Val339Ile	rs559727962, COSM368620	Uncertain significance

HGVSc - DNA level variant description, HGVSp - protein lever variant description, gnomAD AF – variant frequency found in the gnomAD database, dbSNP ID – identifier in NCBI dbSNP or COSMIC databases.

5. Conclusion

Papillary growth pattern in ccRCC is not uncommon and in fact it can constitute a substantial portion the tumor. Papillary RCC with clear cells and MiT family (TFE3/XP11.2) translocation RCCs are the major differential diagnostic considerations, which can be resolved with help of IHC and basic FISH testing. Our NGS molecular analysis supported classifying such tumors as a rare variant of ccRCC.

Disclosure of conflict of interest

All authors declare no conflict of interest.

Funding

The study was supported by the Charles University Research Fund (project number Q39) and by the project Institutional Research Fund of University Hospital Plzen (FN 00669806).

References

[1] Moch H, Cubilla AL, Humphrey PA, Reuter VE, Ulbright TM. The 2016 WHO classification of tumours of the urinary system and male genital organs-part A: renal, penile, and testicular tumours. Eur Urol 2016;70:93–105.
[2] Val-Bernal JF, Salcedo W, Val D, Parra A, Garijo MF. Mucin-secreting clear cell renal cell carcinoma. A rare variant of conventional renal cell carcinoma. Ann Diagn Pathol 2013;17:226–9.
[3] Williamson SR, Kum JB, Goheen MP, Cheng L, Grignon DJ, Idrees MT. Clear cell renal cell carcinoma with a syncytial-type multinucleated giant tumor cell component: implications for differential diagnosis. Hum Pathol 2014;45:735–44.
[4] Tanas Isikci O, He H, Grossmann P, Alaghehbandan R, Ulamec M, Michalova K, et al. Low-grade spindle cell proliferation in clear cell renal cell carcinoma is unlikely to be an initial step in sarcomatoid differentiation. Histopathology 2018;72:804–13.
[5] de Peralta-Venturina M, Moch H, Amin M, Tamboli P, Hailemariam S, Mihatsch M, et al. Sarcomatoid differentiation in renal cell carcinoma: a study of 101 cases. Am J Surg Pathol 2001;25:275–84.
[6] Lopez JI, Angulo JC. Pathological bases and clinical impact of intratumor heterogeneity in clear cell renal cell carcinoma. Curr Urol Rep 2018;19:3.
[7] Salama ME, Worsham MJ, DePeralta-Venturina M. Malignant papillary renal tumors with extensive clear cell change: a molecular analysis by microsatellite analysis and fluorescence in situ hybridization. Arch Pathol Lab Med 2003;127:1176–81.
[8] Diegmann J, Tomiuk S, Sanjmyatav J, Junker K, Hindermann W, von Eggeling F. Comparative transcriptional and functional profiling of clear cell and papillary renal cell carcinoma. Int J Mol Med 2006;18:395–403.
[9] Klatte T, Said JW, Seligson DB, Rao PN, de Martino M, Shuch B, et al. Pathological, immunohistochemical and cytogenetic features of papillary renal cell carcinoma with clear cell features. J Urol 2011;185:30–5.
[10] Haudebourg J, Hoch B, Fabas T, Cardot-Leccia N, Burel-Vandenbos F, Vieillefond A, et al. Strength of molecular cytogenetic analyses for adjusting the diagnosis of renal cell carcinomas with both clear cells and papillary features: a study of three cases. Virchows Arch 2010;457:397–404.
[11] Lek M, Karczewski KJ, Minikel EV, Samocha KE, Banks E, Fennell T, et al. Analysis of protein-coding genetic variation in 60,706 humans. Nature 2016;536:285–91.
[12] Landrum MJ, Lee JM, Benson M, Brown GR, Chao C, Chitipiralla S, et al. ClinVar: improving access to variant interpretations and supporting evidence. Nucleic Acids Res 2018;46:D1062–7.
[13] Gerlinger M, Catto JW, Orntoft TF, Real FX, Zwarthoff EC, Swanton C. Intratumour heterogeneity in urologic cancers: from molecular evidence to clinical implications. Eur Urol 2015;67:729–37.
[14] Rotterova P, Martinek P, Alaghehbandan R, Prochazkova K, Damjanov I, Rogala J, et al. High-grade renal cell carcinoma with emperipolesis: clinicopathological, immunohistochemical and molecular-genetic analysis of 14 cases. Histol Histopathol 2018;33:277–87.
[15] Faragalla H, Al-Haddad S, Stewart R, Yousef GM. The significance of florid giant cell component in renal cell carcinoma: a case report and review of the literature. Can J Urol 2010;17:5219–22.
[16] Fuzesi L, Gunawan B, Bergmann F, Tack S, Braun S, Jakse G. Papillary renal cell carcinoma with clear cell cytomorphology and chromosomal loss of 3p. Histopathology 1999;35:157–61.
[17] Moch H, Humphrey PA, Ulbright TM, Reuter VE. WHO Classification of Tumours of the Urinary System and Male Genital Organs. Lyon: IARC; 2016.
[18] Hes O, Comperat EM, Rioux-Leclercq N. Clear cell papillary renal cell carcinoma, renal angiomyoadenomatous tumor, and renal cell carcinoma with leiomyomatous stroma relationship of 3 types of renal tumors: a review. Ann Diagn Pathol 2016;21:59–64.
[19] Jia LJG, Al-Ahmadie H, Fine SW, Gopalan A, Sirintrapun SJ, Tickoo S, et al. Clear cell renal cell carcinoma with prominent papillary architecture: a rare morphologic variant supported by molecular evidence. Lab Invest 2018;98:353.
[20] Network CGAR. Comprehensive molecular characterization of clear cell renal cell carcinoma. Nature 2013;499:43–9.